Supplementary Materials for

Spontaneous activity competes with externally evoked responses in sensory cortex.

Golan. Karvat, Mansour Alyahyay, Ilka Diester.

Correspondence to: ilka.diester@biologie.uni-freiburg.de

This PDF file includes:

Figs. S1 to S9

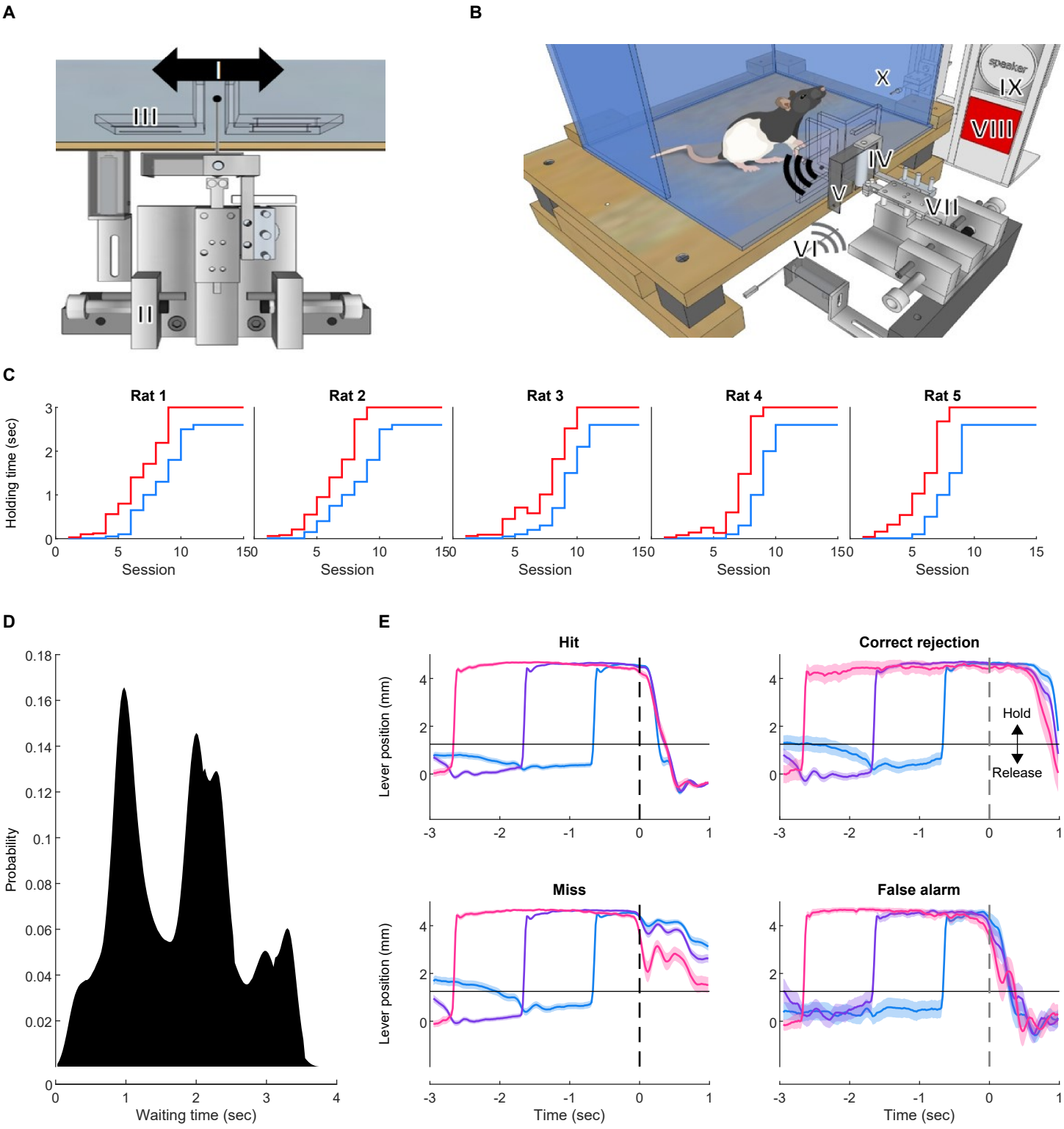

Fig. S1. Vibrotactile detection task for freely moving rats.

A. Manipulandum. The rat had to hold the lever (I) and pull it in its preferred direction against the force of the centering magnets (II). The lever was enclosed between two walls (III) ensuring uni-manual manipulation.

B. Complete setup. The cage was made of glass and located on a wooden surface, ensuring isolation from ground and reduced static discharge. After the holding-time, a vibrotactile stimulus was conveyed via a Piezo actuator (IV), signaling the rat to release the lever. The actuator was shielded electrically (V) to avoid electromagnetic noise in electrophysiological recordings. In a subset of trials, another shielded actuator (VI) was activated as a control. A strain gauge (VII) was used to detect the touch and to calibrate the vibration amplitude. VIII- Red cage light. IX- speaker used to deliver a clicker tone in a correct trial and white noise after errors. X- reward-delivery spout.

For early training stages, we used additional 4 individually-controlled setups for simultaneous training. Each setup included a 30x25x30 cm Plexiglas box with a grounded metal floor. The metal lever was covered with a 7

mm (diameter) metal ball. The metal holder was connected via a high (0.5 GOhm) resistance to a 5V source, thus forming a conductive touch sensor. To deliver vibrotactile stimuli, we glued a small vibrating motor (3V ERM motor) to the lever. The vibrator, touch sensor, and angle encoder were controlled by an Arduino Uno connected via TTL to the Med Associates control cabinet.

C. Holding duration training progress of 5 rats. Rats had to hold the lever passed the threshold position for at least the holding time to obtain a reward. Blue lines indicate the holding duration at the beginning of each session. The holding duration was incremented automatically in small steps, until reaching the duration indicated by the red line.

D. Holding duration during the vibro-tactile detection task. The holding time was pseudo-randomized between 600, 1600 and 2600 ms, with a 4:4:1 ratio (note the tri-modal holding-time distribution). N=4,225 trials, 25 sessions.

E. Mean ± 95% confidence interval of the lever position (measured by the angle encoder). Time t=0 indicates the stimulus onset. Horizontal line at ~1mm indicates the hold/ release threshold. Trials with holding time = 600 ms are indicated in blue, 1600 ms in purple and 2600 ms in pink.

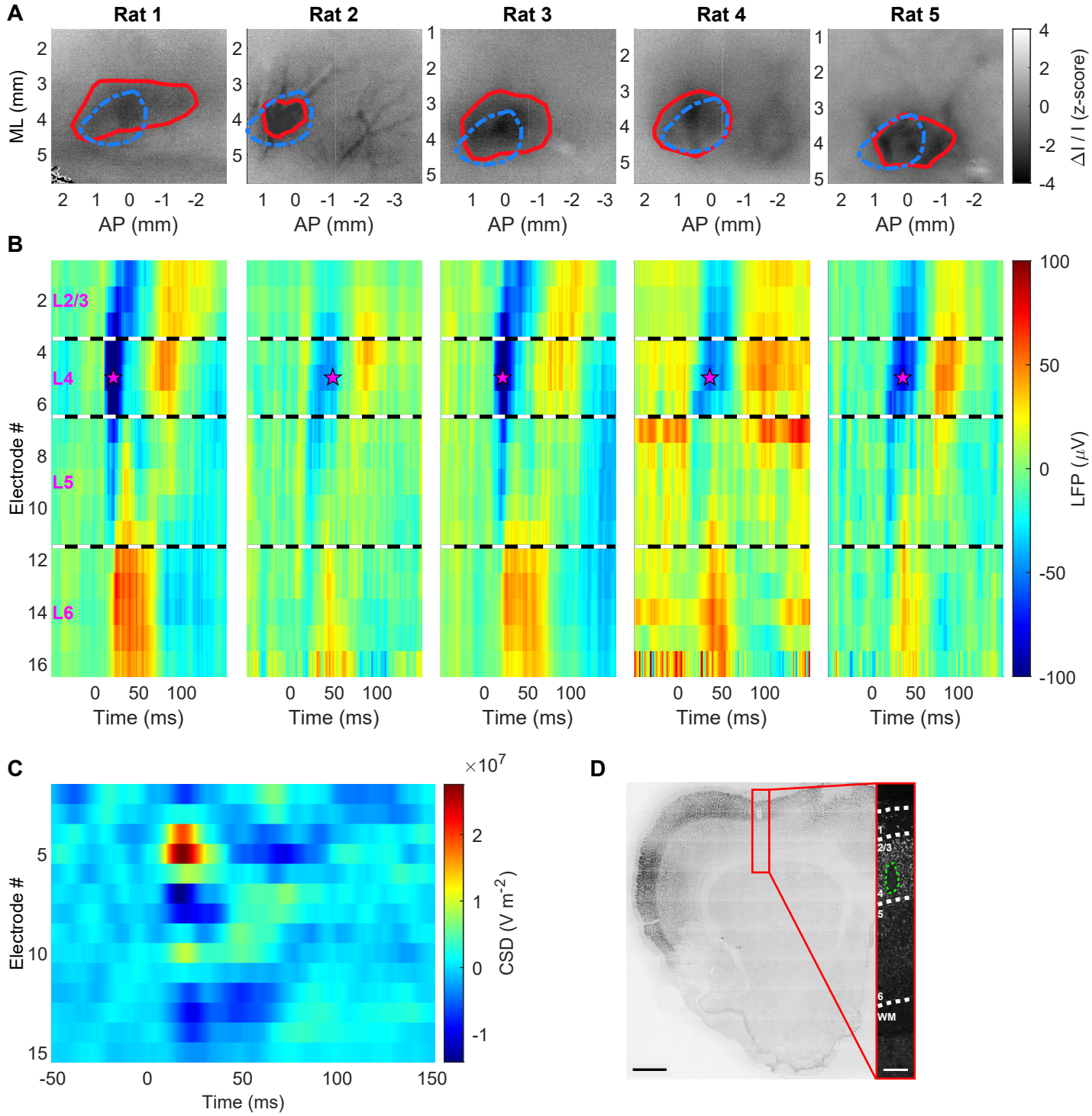

Fig. S2. Implant localization.

A. Intrinsic signal imaging from 5 rats. The images represent the difference in absorption intensity of 855 nm light between vibration trials and blank (no vibration) trials, relative to baseline absorption (ΔI / I) and z-normalized. Blue dashed line: assumed SI forepaw location based on published somatotopic maps (26). Red lines: responsive area. ML: medial-lateral direction. AP: anterior-posterior.

B. ERP maps of each rat. Magenta star indicates minimal LFP (maximal depolarization) and black and white dashed lines indicate assumed borders between cortical layers.

C. Current-sink density (CSD) map computed as the second spatial derivative of the LFP and averaged over rats. Time $t = 0$ indicates stimulus onset.

D. Left, coronal section (10x) of an explanted brain after electrical lesion and NeuN staining. Area marked in red is shown on the right with higher magnification (20x). White dashed lines: estimated borders between layers. Green: lesion. Numbers: cortical layers. WM: white matter. Scale bars: left, 1000 μm, right, 200 μm.

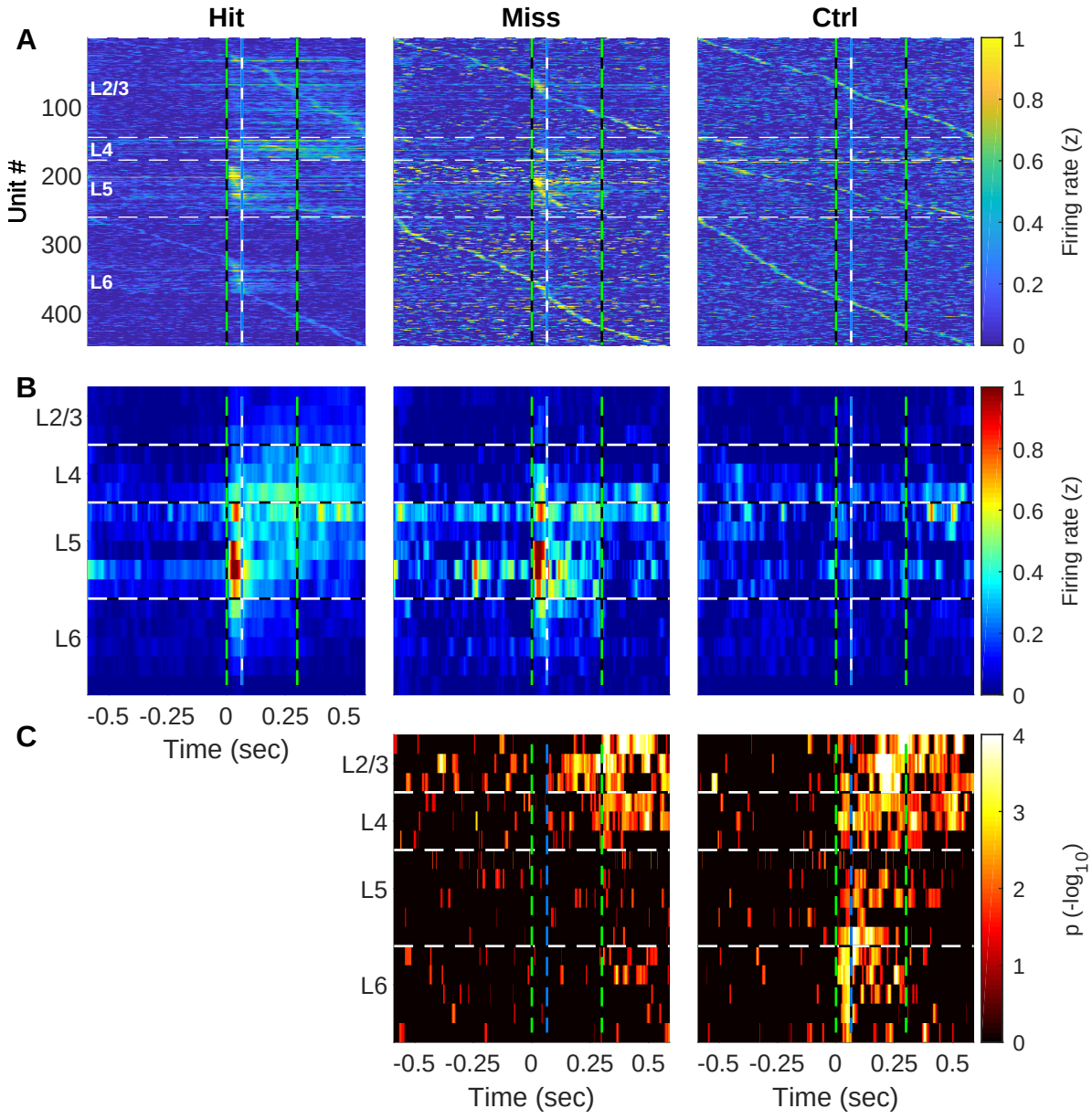

Fig. S3. Laminar characterization of firing rate.

A. FR of each unit (N=447 units in 10 sessions from 5 rats) during hit (left), miss (middle) and catch (right) trials. Units are sorted according to layer and timing of maximal FR. Black and white lines denote estimated limits between layers. Black and green lines denote the stimulus onset (t = 0) and offset (t = 0.3). White and blue lines: ERP phase change from de- to hyper-polarization (t = 0.065).

B. Mean FR per electrode.

C. *P*-values from statistical comparisons (two-sided *t*-test) between hit and miss (middle) and hit and control (right). Non-significant (p>0.05) time points appear in black. At stimulus onset (initial 65 ms, blue dashed line) there is a difference between hit and control, but not between hit and miss. The difference between hit and miss begins at L2/3 65 ms after stimulus onset (when the ERP changes from de- to hyper-polarization). At L4 the conditions differ after stimulus offset (0.3 sec, green dashed line).

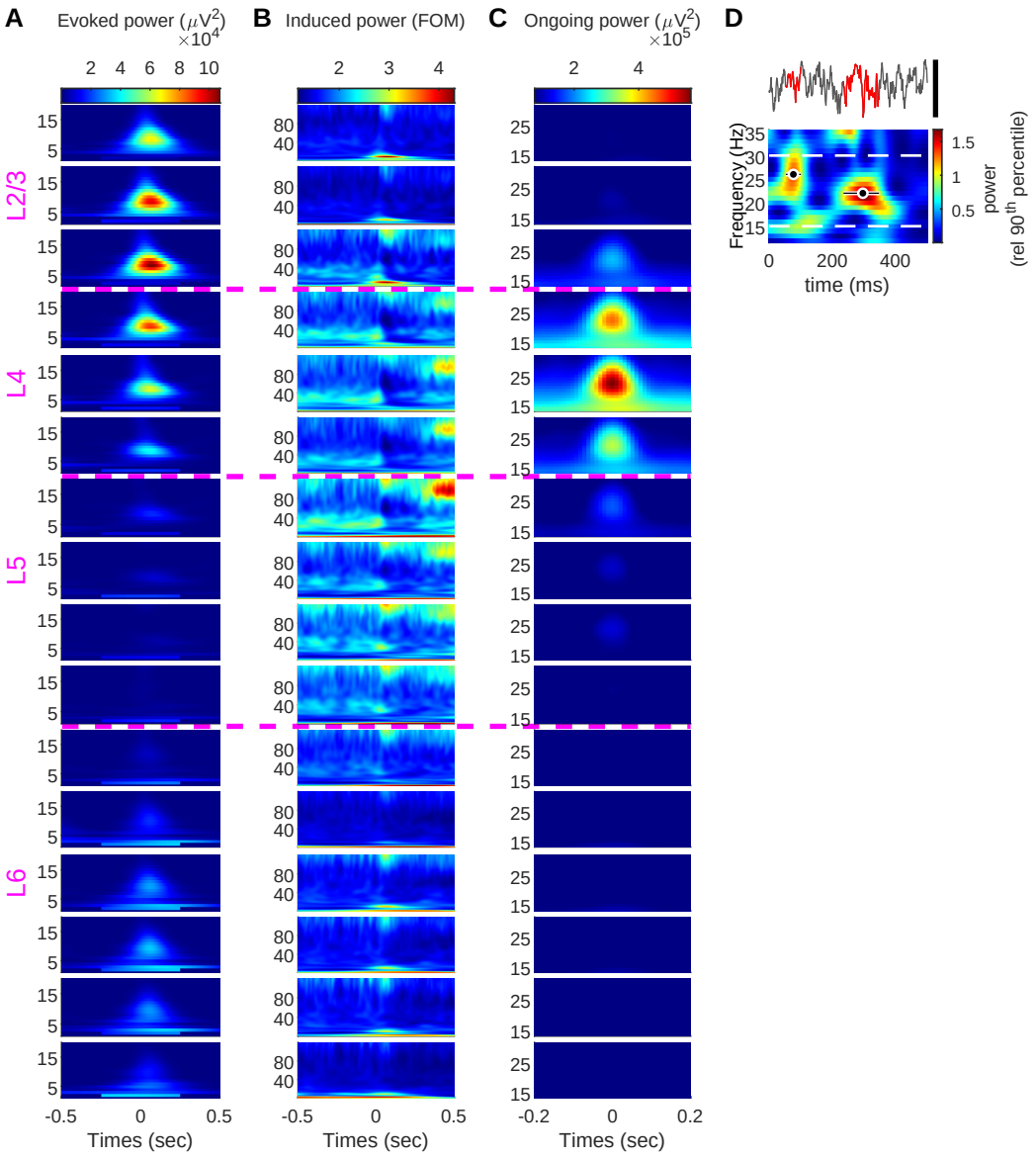

Fig. S4. Laminar characterization of evoked, induced and ongoing oscillations.

A. Time frequency representation (TFR) per channel of the evoked oscillations, computed by averaging the raw LFP time-locked to the stimulus, and then transferring to the frequency domain by Morlet wavelets. Numbers in magenta denote cortical layers, numbers in black the frequency in Hz. Dashed magenta lines (**A-C**) indicate estimated cortical layer borders. Time $t = 0$ indicates stimulus onset.

B. TFR of the induced oscillations, computed by first transferring to the frequency domain by Morlet wavelets, normalizing to the median of each frequency and then averaging over trials. FOM, fraction of the median. Time $t = 0$ indicates stimulus onset.

C. Example of localization of beta-band ongoing oscillation bursts. Time $t = 0$ indicates burst power maxima detected on electrode 5 (the reference electrode).

D. Exemplary oscillatory bursts. Upper panel: raw LFP trace. Bursts are indicated in red. Scale bar, 0.5 mV. Lower panel: TFR of the trace on top. Bursts were defined as local maxima in the time-frequency plane, higher than the 90th percentile of the peak frequency (black dots). Burst-occupancy was defined as the duration around the peak in which the power in the peak frequency exceeded the threshold. White dashed lines: limits of the beta band.

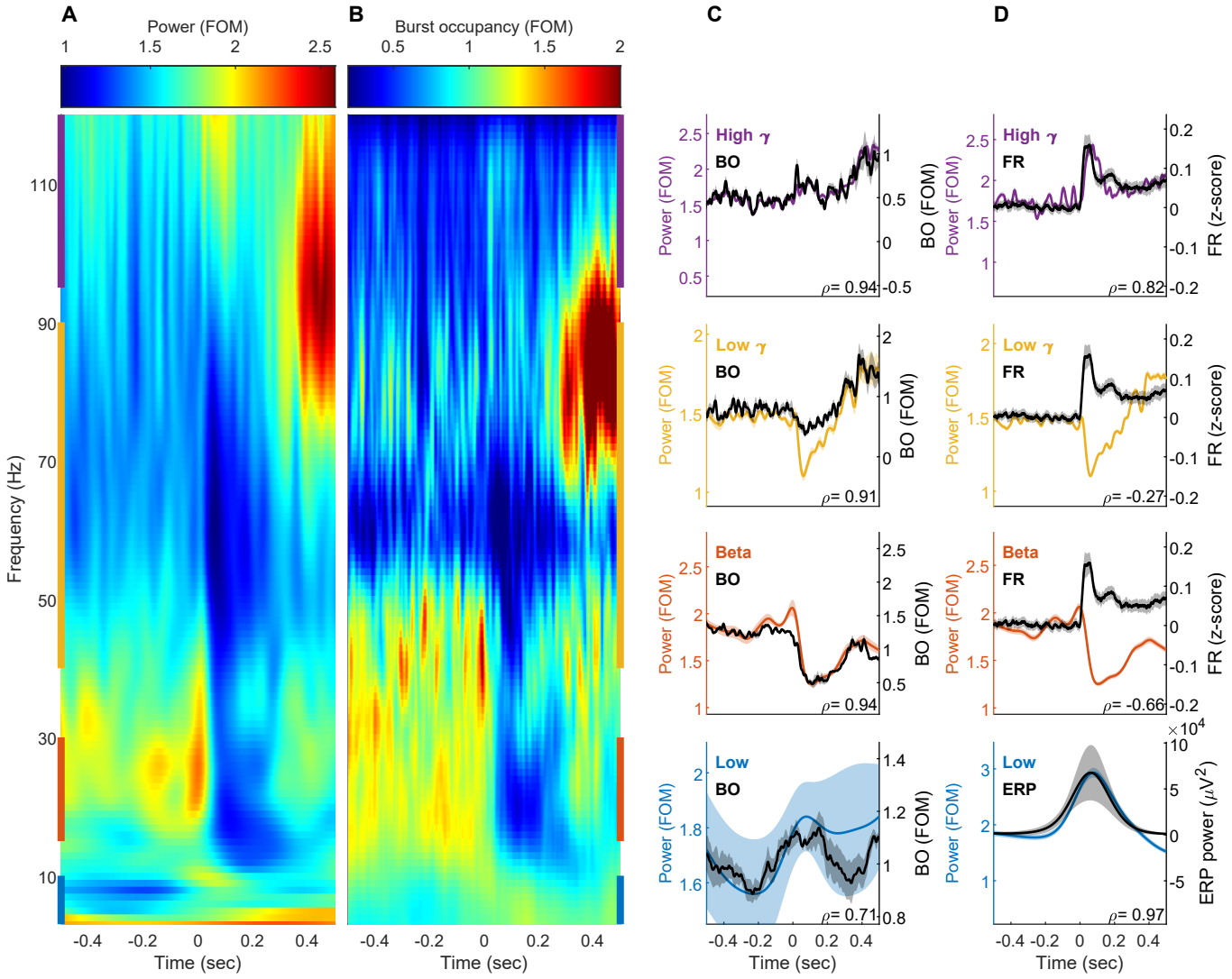

Fig. S5. Power dynamics are correlated with burst activity and correlated to externally-driven signal in a band-dependent manner.

A-C. Power dynamics and burst occupancyare strongly correlated for all frequencies >15 Hz. **A**. Power spectrogram, computed by transforming the LFP to the frequency domain using Morlet wavelets, normalizing to the median per frequency and averaging over hit trials. Colored lines on the left refer to band limits corresponding to color code in **C** and **D**. In all panels, time $t = 0$ indicates stimulus onset. **B**. Occupancyof bursts, defined similarly to the online burst occupancydetection algorithm, as time points with power in a certain frequency higher than the frequency above and the frequency below (in steps of 1 Hz) and higher than the 90th percentile per frequency. The number of burst time points was averaged over hit trials and normalized to the median of each frequency. **C.** Power (averaged over frequencies ± 95% confidence interval indicated as shaded areas) per band with violet referring to high gamma, yellow to low gamma, orange to beta, and blue to low frequencies. Black refers to mean ± 95% confidence interval of the burst occupancy (BO). ρ denotes Pearson's correlation coefficient. All data in **A-C** were recorded on electrode 5 (L4).

D. LFP power correlation with externally driven signal is layer- and band-specific. Colored lines: power dynamics in L4 (electrode 5) for beta and low gamma, and in L2/3 (electrode 2) for high gamma and low frequencies. Black: Normalized population firing-rate (FR, for high gamma, low gamma and beta) or the TFR of the ERP in L2/3 (channel 3, for low frequencies).

FOM, fraction of the median, BO, burst occupancy, FR, population firing rate.

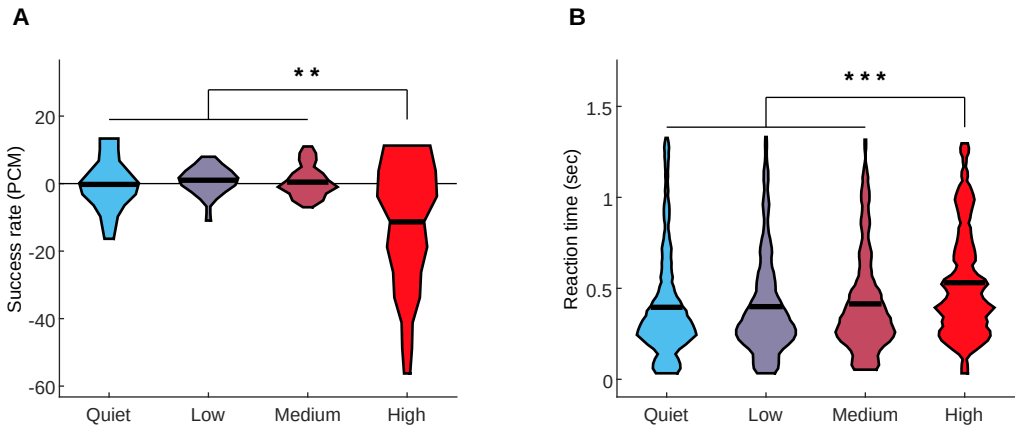

Fig. S6. Trial-by-trial impact of beta-burst occupancy on detection.

Effect of categorical segregation of beta-burst occupancies per trial on percent change from the mean (PCM) of success rate (**A**) and reaction time (**B**). Quiet: no bursts during holding-time (HT). Low: less than a quarter of HT includes bursts. Medium: quarter to half the HT includes bursts. High: more than half the HT includes bursts. The widths of the shapes in **A** indicate distribution of sessions (N=10 from 5 rats), and in **B** the distribution of trials (N= 425, 1006, 510 and 138 for quiet, low, medium and high burst occupancies , respectively). Black horizontal lines indicate the mean. Main effects: **A.** $F_{3,83}$= 6.68, p= 4.3*10^{-4}; **B.** $F_{3,2075}$= 10.43, p= 8.29*10^{-7}. ** - p<0.01, *** - p<0.001, ANOVA with Tukey's post-hoc.

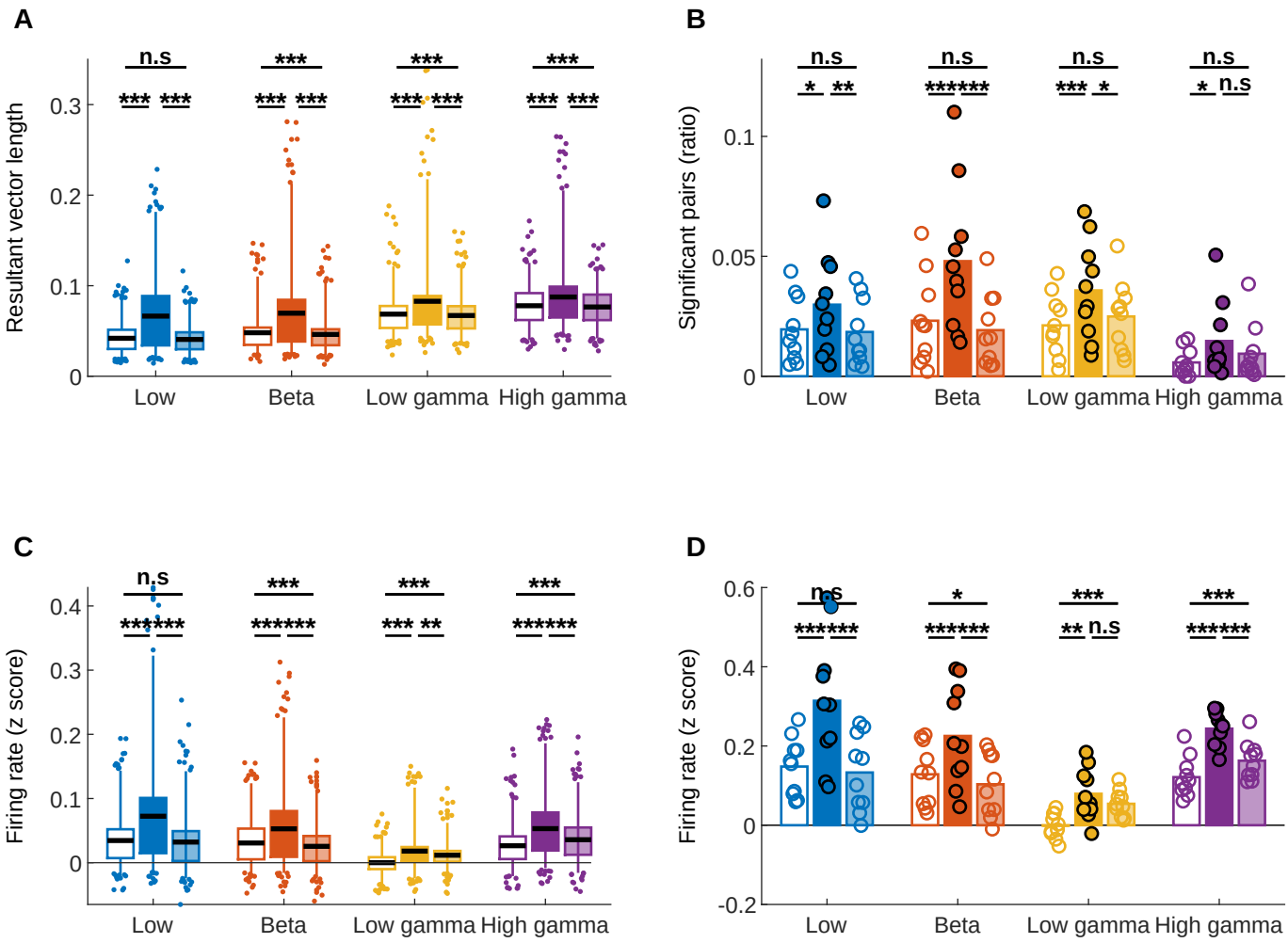

Fig. S7. Modulation of unit activity in and out of bursts

Comparison of spike-field coherence (A), pair-wise synchrony (B) and FR of single units (C) and of the entire population recorded per session (D) during bursts in different bands (filled bars) and time-matched epochs immediately before (empty bars) or after (transparently filled bars) the bursts. Main effects of time (before, during or after burst) in ANOVA for repeated-measures: A: $F_{11,4895} = 127.41$, $p = 3.72*10^{-26}$. B: $F_{2,72} = 56.5$, $p = 6.97*10^{-9}$. C: $F_{2,3632} = 808.3$, $p = 2.19*10^{-147}$. D: $F_{2,72} = 102.11$, $p = 4.7*10^{-12}$. For each band, the top significance line denotes comparison between before burst to after burst in a post-hoc analysis with Tukey's adjustment, bottom-left comparison between before and burst and bottom-right comparison between burst and after. *- $p < 0.05$, **- $p < 0.01$, ***- $p < 0.001$, n.s- not significant.

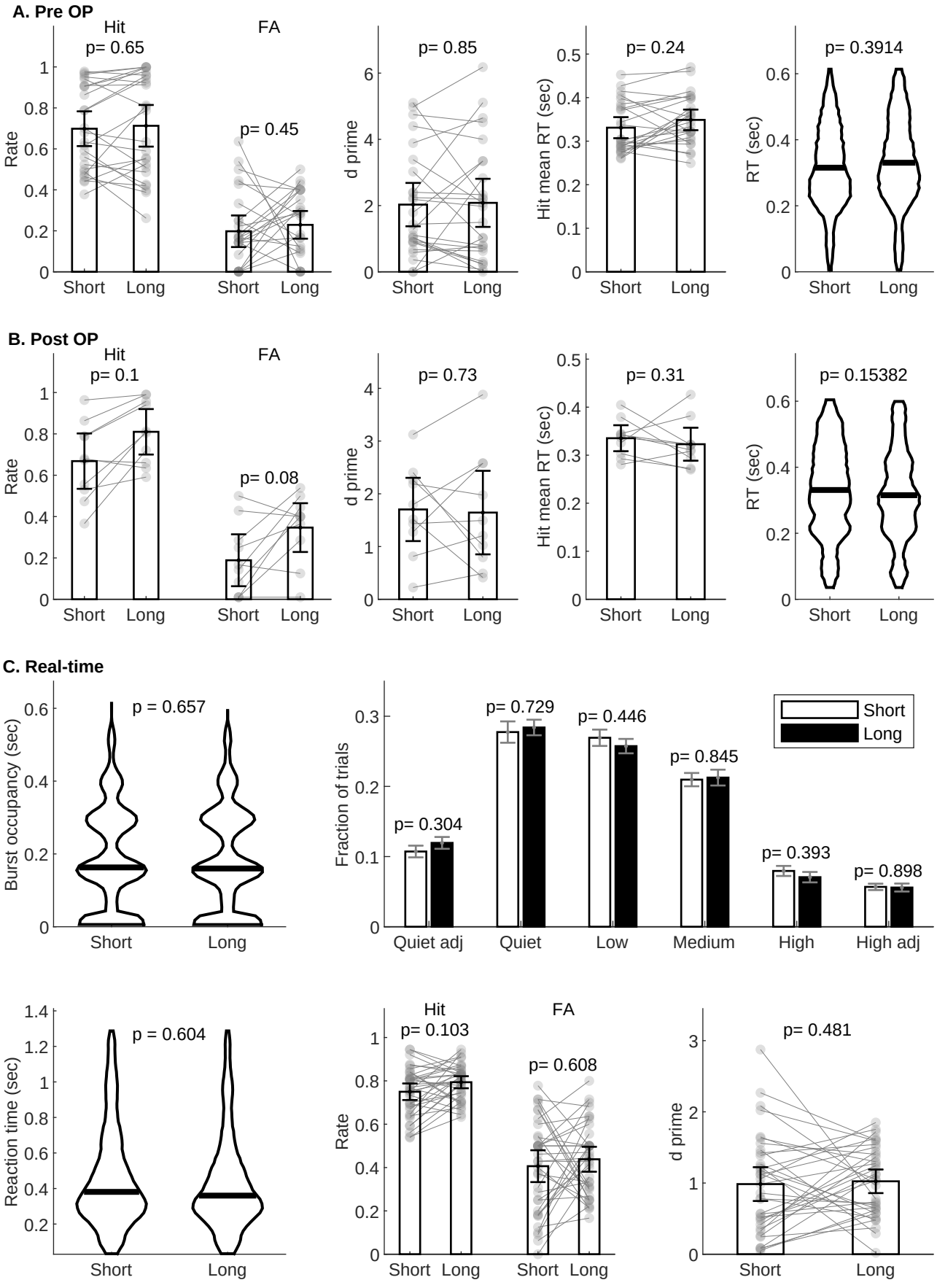

Fig. S8. Pre-stimulus waiting time has no significant effect on detection

Comparison of behavioral parameters in trials with short (600 ms) and long (1600 ms) waiting times before surgery (A, N=25 sessions), after surgery (B, N=10) and at the real-time experiment sessions (N=35). *p* indicates the result of a two-sided Wilcoxon rank-sum test, except for C. Fraction of trials, in which the results of a 2-way repeated-measures ANOVA with Tukey's posthoc tests are presented. FA; false-alarm. RT; reaction time. adj.; real-time adjusted amplitude

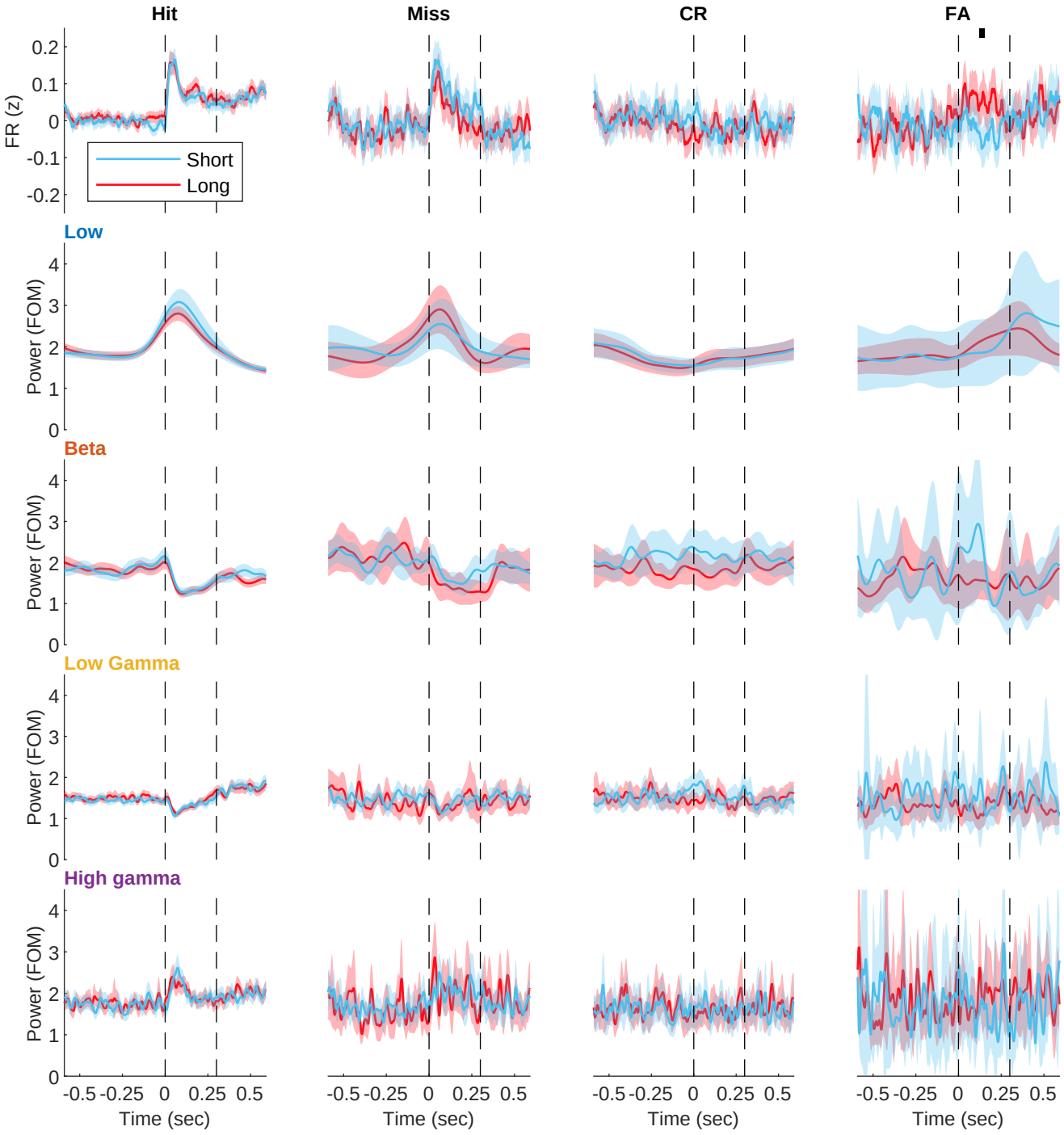

Fig. S9. Pre-stimulus waiting time has no significant effect on FR and LFP-power

Comparison of firing-rate and LFP power in different frequency bands in trials with short (600 ms) and long (1600 ms) waiting times, aligned to stimulus presentation times (dashed black lines). The black bar above the graph of FR in FA trials indicates a time-bin with a difference between short and long trials in a 2-way repeated measures ANOVA with Tukey's posthoc. Main effects for interaction between time and waiting-time duration: FR: $F_{440,\ 214080} = 3.25$, $p = 1.93*10^{-4}$. Low: $F_{429,\ 42822} = 3.27$, $p = 2.0*10^{-4}$. Beta: $F_{429,\ 42822} = 1.27$, $p = 0.24$. Low-Gamma: $F_{429,\ 42822} = 1.4$, $p = 0.17$. High-Gamma: $F_{429,\ 42822} = 1.01$, $p = 0.44$.